Journal of Molecular Liquids 328 (2021) 115457

Contents lists available at ScienceDirect

Journal of Molecular Liquids

journal homepage: www.elsevier.com/locate/molliq

Synthesis, characterization, antimicrobial, BSA binding, DFT calculation, molecular docking and cytotoxicity of Ni(II) complexes with Schiff base ligands

J. Jeevitha Rani [a], A. Mary Imelda Jayaseeli [a,*], S. Rajagopal [b], S. Seenithurai [c], Jeng-Da Chai [c,d], J. Dhaveethu Raja [e], R. Rajasekaran [f]

[a] Research Center of Chemistry, Jayaraj Annapackiam College for Women(Autonomous), Mother Teresa Women's University, Kodaikanal, Periyakulam, Theni, Tamil Nadu 625601, India
[b] School of Chemistry, Madurai Kamaraj University, Madurai, Tamil Nadu 625021, India
[c] Department of Physics, National Taiwan University, Taipei 10617, Taiwan
[d] Center for Theoretical Physics and Center for Quantum Science and Engineering, National Taiwan University, Taipei 10617, Taiwan
[e] Department of Chemistry, The American College, Tallakkulam, Madurai, Tamil Nadu 625002, India
[f] School of Biosciences and Technology, VIT University, Vellore, Tamil Nadu 632014, India

ARTICLE INFO

Article history:
Received 15 August 2020
Received in revised form 16 January 2021
Accepted 20 January 2021
Available online 23 January 2021

Keywords:
Ni(II) Schiff base complexes
Antimicrobial
BSA binding
Molecular docking
Cytotoxicity

ABSTRACT

A series of a tetradentate N_2O_2 Schiff base ligands (**1a-e**), [N,N′-(X)bis(salicylidene)1,2-phenylenediamine], salphens {where X = H (**1a**), Cl (**1b**), Br (**1c**), CH_3 (**1d**), OCH_3(**1e**)} were synthesized from condensation of substituted salicylaldehydes with 1,2-phenylenediamine and nickel(II) complexes(**2a-e**) from corresponding Schiff base ligands(**1a-e**). The stoichiometric ratios of the prepared ligands (**1a-e**) and their Ni(II)-salphen complexes (**2a-e)** were structurally characterized by various analytical and spectroscopic techniques such as ^{1}H NMR, FT-IR, mass, UV–visible, PXRD, magnetic moments and molar conductivity measurements. These results suggest that Ni(II)-salphen complexes (**2a-e)** have square planar geometry. The molar conductivity measurements indicate that all complexes (**2a-e)** are non-electrolytes. Density Functional Theory (DFT) calculations have been used to investigate the optimized structure and chemical reactivity of these Ni(II) complexes(**2a-e**) from their Frontier Molecular Orbitals (FMO). The binding capabilities of the Ni(II) Schiff base complexes (**2a-e**) with Bovine Serum Albumin (BSA) have been studied through electronic absorption, fluorescence and cyclic voltammetric methods. Further the nature of interaction of Ni(II) complexes (**2a-e**) towards BSA were confirmed using molecular docking analyses. All these results demonstrated that the Ni(II) complexes **2d** and **2e** have better binding affinity towards BSA among all the Ni(II) complexes. The antimicrobial studies reveal that the Ni(II)-salphen complexes (**2a-e**) have higher inhibitory effect than ligands (**1a-e**) against the selected pathogenic microorganisms. Furthermore, in vitro cytotoxicity of ligands (**1a-e**) and Ni(II) complexes(**2a-e)** were evaluated by MTT assay against MCF-7. The observed IC_{50} values against MCF-7 cell lines suggest that Ni(II) complexes(**2a-e)** show more significant anticancer activity than their corresponding ligands(**1a-e**)**.** It is explored that complexes **2d** and **2e** bearing electron donating groups have greater anticancer potency. Comparison of our results with cisplatin, Zn(II)-salphen and V(IV)-salphen complexes indicated that Ni(II)-salphen complexes can be considered as the potential candidates for use as effective anticancer agent in future.

1. Introduction

For the past few decades, cancer is one of the most fatal diseases in the world and thus much devoted research in the development of drugs is required. The discoveries of cis-platin and related platinum-based drugs are the milestone in the treatment of the several types of cancer and serve as chemotherapeutic agents [1–3]. However, they have several serious side effects including nephrotoxicity, ototoxicity and high toxicity acquired resistances which restrict their clinical applications [4–6]. Therefore, considerable efforts to improve the efficacy and overcome these drawbacks stimulated the development of new anticancer drugs based on transition metal complexes [7,8]. Among the transition metals, nickel is a biologically relevant element in group 10, the same chemical group as platinum. Nickel(II) complexes with ligands possessing nitrogen and sulphur donor ligands are highly significant [9–12] because several hydrogenases and carbon monoxide dehydrogenases [13] contain nickel ion as their active site. Recently, nickel

* Corresponding author at: Research Center of Chemistry, Jayaraj Annapackiam College for Women (Autonomous), Periyakulam, Theni 625601, Tamil Nadu, India.
E-mail address: imeldachem@annejac.ac.in (A.M.I. Jayaseeli).

https://doi.org/10.1016/j.molliq.2021.115457
0167-7322/

complexes have been widely investigated owing to their various properties with potential biological and clinical applications, such as DNA and protein interactions, antioxidant, antimicrobial activities and antiproliferative agents [14–17]. Recent literature data show that nickel complexes have been designed and developed as anticancer drugs with potent therapeutic properties [18–22].

Especially, metal complexes with tetradentate Schiff base ligands like salen[*N*,*N*′-bis(salicylidene)ethylenediamine] and salphen [*N*,*N*′′-bis(salicylidene)1,2-phenylenediamine] have attracted significant attention in many researchers due to their straightforward synthesis, structural liability, diverse effect in configuration and sensitivity [23–25]. Potential applications of salphen based metal complexes, particularly therapeutic agents and biological activities, encouraged us to continue our studies on these types of complexes [26–29].

Recent literature reports reveal that transition metal complexes have been extensively utilized as the probes for proteins and as chemotherapeutic agents [30]. Among the serum albumins, Bovine Serum Albumin (BSA) is one of the most abundant water soluble proteins and has many physiological functions [31]. BSA is usually selected as model protein, due to its structural similarity with Human Serum Albumin (HSA), its low cost and wide availability [32,33]. The formation of drug-protein adduct as a stable protein complex has important effect on the distribution, absorption, metabolism and properties of drugs. Such interactions of drug compounds carrying aromatic rings are very important for protein sterilization and different.

regulation processes [34]. Consequently, the interaction of metal complexes towards protein BSA is very much useful in the design and synthesis of metal-based anticancer therapeutics. Some recent reports indicate the importance of some metal-Schiff base complexes as anticancer agents and sensors [35].

Thus, the present study focuses on the synthesis and investigation of five Ni(II) complexes(**2a-e**) containing Schiff base ligands **(1a-e)** towards their effectiveness as anticancer and antimicrobial agents. The structures of the prepared complexes have been characterized by various spectroscopic techniques. The DFT calculations were performed to check the molecular interactions in a compound and its stability. All the synthesized compounds have been evaluated using different experimental techniques to assess their binding ability with BSA, antimicrobial and cytotoxicity potential. Molecular docking studies were also carried out for all the complexes to estimate their binding affinity with BSA.

2. Experimental

2.1. Materials and instrumentation

Salicylaldehyde and 1,2-phenylenediamine were purchased from Central Drug House(P) Ltd. 5-chloro salicylaldehyde, 5-bromo salicylaldehyde, 5-methyl salicylaldehyde and 5-methoxy salicylaldehyde were acquired from Sigma Aldrich in pure form. Nickel chloride hexahydrate was received from MERCK and BSA from Sisco Research Laboratories Pvt. Ltd. and used without further purification.

The conductivity measurements were measured on Deluxe 601 conductivity meter. Elemental analyses (C, H, N and S) were performed by using Vario EL III analyzer. Magnetic susceptibility of the complexes was measured by MSB mark 1 Sherwood U.K. The UV–visible absorption spectra have been recorded using UV-1800 Shimadzu spectrophotometer. The infrared spectra were recorded in Shimadzu FT-IR spectrometer, in solid phase using KBr pellets. ^{1}H NMR for the Schiff base ligands have been acquired on a Bruker 300 MHz NMR spectrometer in DMSO-d_6 solution using TMS as the internal standard. The mass spectra were recorded by JEOL SX-102A spectrometer. Powder X-ray diffraction measurements were performed on a Rigaku Miniflux-600 X-ray diffractometer. The emission spectra were recorded on a JASCO FP-6200 spectrofluorimeter. Electrochemical studies were carried out using a CHI-608E instrument.

2.2. Synthesis of Schiff base ligands (*1a-e*)and Ni(II)-Schiff base complexes (*2a-e*)

The Schiff base ligands (**1a-e**) and Ni(II)-Schiff base complexes(**2a-e**) were synthesized by reported procedures [27,29]. Among the synthesized compounds, complexes **2a**, **2c**, **2e** were known [26,28,36] and complexes **2b** and **2d** were newly synthesized. The synthetic protocols for the preparation of Ni(II)-Schiff base complexes (**2a-e**) were shown in Scheme 1.

2.2.1. Synthesis nickel(II) complexes *2b* and *2d*

The nickel(II) complexes **2b** and **2d** were synthesized by the reaction of stoichiometric amounts of the appropriate ligand **1b** and **1d** (4 mmol) with nickel chloride hexahydrate (4 mmol) in 1:1 ratio in an ethanolic medium. The resulting mixture was refluxed under stirring for 2 h and then cooled to room temperature. The precipitated complexes were filtered, washed with ethanol and finally dried in vacuum.

Ni(II) complex **2b**: Color: Reddish brown, Yield: 67%, Λ_c: 17 Ω^{-1} cm^{2} mol^{-1}, IR (KBr) ν/cm^{-1}: 3393(ν -OH), 1605 (ν C=N), 1329 (ν C–N), 560 (ν –M-O), 461(ν –M-N), UV–visible (λ_{max}): 380, 482 nm, Mass: 442 (*m*/*z*), Anal. Cacld(%) for $C_{20}H_{12}O_2N_2Cl_2Ni$: C, 54.13; H, 2.64; N, 6.31, Found (%):C, 54.29; H, 2.71; N, 6.34.

Ni(II) complex **2d**: Color: Dark Brown, Yield: 63%, Λ_c: 21 Ω^{-1} cm^{2} mol^{-1}, IR (KBr) ν/cm^{-1}: 3386 (ν -OH), 1612 (ν C=N), 1345 (ν C–N), 540 (ν –M-O), 440(ν –M-N), UV–visible (λ_{max}): 376, 485 nm, Mass: 401 (*m*/*z*), Anal. Cacld(%) for $C_{22}H_{18}O_2N_2Ni$: C, 65.75; H, 4.32; N, 6.91, Found (%): C, 65.83; H, 4.48; N, 6.98.

2.3. Computational methods

The most versatile computational methods featured in Q-Chem 4.4 [37] were adopted for DFT calculations. The evaluation was performed by aug-cc-pVDZ basis set for **2c** and cc-pVTZ basis set [38] for all other complexes (**2a,b, d** and **e**). Kohn-Sham density functional theory (DFT) was employed with SCAN0 hybrid meta-GGA exchange-correlation functional (which contains 25% Hartree-Fock exchange, 75% SCAN exchange, and 100% SCAN correlation) [39,40]. An ultrafine grid containing 99 Euler-Maclaurin radial grid points and 590 Lebedev angular grid points were used to execute the spin-restricted and spin-unrestricted calculations of Ni(II) complexes.

2.4. Stability determination

The stability of the Ni(II) complexes have been analyzed by UV–visible absorption spectra . The stock solutions of the complexes (1×10^{-6}M) in Tris-HCl buffer (pH 7.4) were prepared in CH_3CN and the spectra were monitored at different time intervals over 24 h at 37 °C.

2.5. BSA binding experiments

The binding interaction of Ni(II) complexes (**2a-e)** with BSA have been studied employing absorption, fluorescence and electrochemical measurements. All the experiments were followed in the appropriate medium (70% CH_3CN–30% H_2O (*v*/*v*)) keeping at physiological pH 7.4. A stock solution of BSA was prepared using Tris-buffer and always freshly prepared before use. The absorption spectral titrations were done with fixed Ni(II) complex concentration (2 μM) but varying the BSA concentration (0–18 μM). In a fluorescence method, BSA was excited at 280 nm at room temperature and the emission was monitored at 340 nm. The emission spectra of BSA were recorded in the range of 280-500 nm with increasing amounts of Ni(II) complexes (0–18 μM). The electrochemical studies were carried out by maintaining the Ni(II) complexes at 2 μM concentration as constant and varying the concentration of BSA (0-20 μM) at pH 7.4.

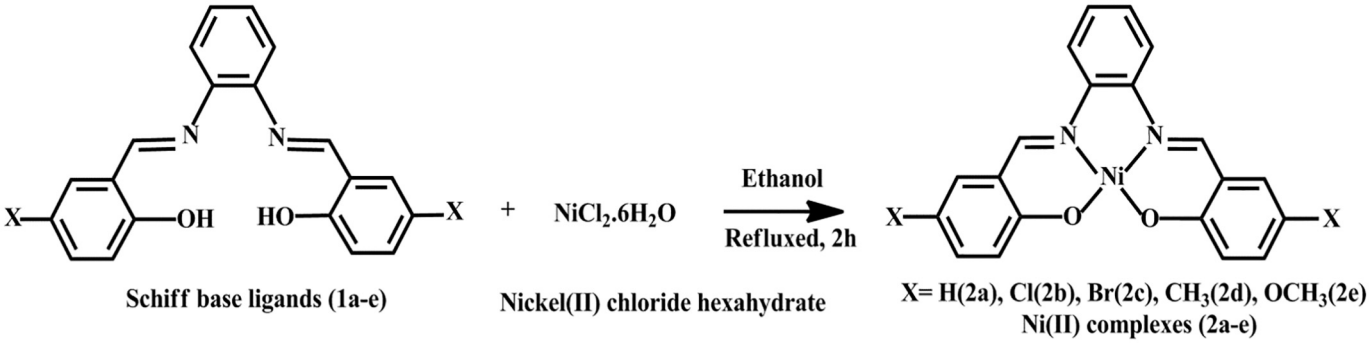

Scheme 1. Synthetic pathway for Ni(II)-Schiff base complexes (**2a-e**)

2.6. Molecular docking studies

Computer molecular docking was used to simulate interactions and evaluate active sites. The docking simulation analyses were performed using the software package Autodock Vina [41]. The BSA (PDB ID: 4F5S) protein three dimensional structures were downloaded from protein data bank (PDB) [42]. The Auto Grid was used to calculate grids and a blind docking with 126 lattice points along X, Y and Z axes.

2.7. Antimicrobial studies

Antimicrobial activities of the Schiff base ligands (**1a-e)** and Ni(II) complexes (**2a-e)** have been tested by well diffusion method. The chosen bacterial strains were *Escherichia coli* (*E.coli*) and *Staphylococcus aureus* (*S. aureus*). The fungi strains were *Aspergillus niger* (*A. niger*) and *Candida albicans* (*C. albicans*). Amikacin and Nystatin were used as the standard antibacterial and antifungal drugs respectively.

2.8. Cytotoxicity studies

The solubility of potential anticancer drug in biological assay buffers is an important factor in order to produce accurate activity in cell-based assays. Hence biological experiments were followed in the appropriate medium keeping (70% CH_3CN–30% H_2O (v/v)) at physiological condition. This condition was typically used to conduct different dilutions of the compounds for screening biological activities.

2.8.1. Cell culture

Human breast cancer cell lines (MCF-7) were cultured at 37 °C in a 5% CO_2 atmosphere in Dulbecco's Modified Eagle's Medium (DMEM) containing 10% Fetal Bovine Serum (FBS), 100 μg/ml penicillin and 100 μg/ml streptomycin as antibiotics.

2.8.2. Cell viability assay

The in vitro anticancer activity of Schiff base ligands (**1a-e)** and Ni(II) complexes (**2a-e)** were studied against MCF-7cell lines by using MTT [3-(4,5-dimethyl-2-thiazolyl)-2,5 diphenyl-2-H-tetrazolium bromide)] assay [43]. The cells were seeded into a 96-well plate at a density of 1×10^6 cells per well and incubated in medium containing Schiff base ligands and Ni(II) complexes at concentrations ranging from 0.5 to 100 μM for 24 h at 37 °C in a humidified atmosphere of 95% air and 5% CO_2**.** Control cultures were treated with DMSO. The cultures were again incubated as above. After 24–36 h, 20 μl of MTT solutions were added to each well and the cultures were further incubated for 4 h and then 200 μl of DMSO were added. The formed crystals were dissolved gently by pipetting two to three times slowly. The absorbance at 570 nm was measured using plate reader. The percentage of viability was calculated using the formula:

$$\%\text{Cell Viability} = \text{Control OD} - \text{sample OD}/\text{control OD} \times 100$$

3. Results and discussion

The formation of Schiff base ligands and Ni(II)-Schiff base complexes were confirmed using the analytical and spectroscopic techniques. The synthesized compounds were found to be solid, soluble in CH_3CN, DMSO and DMF solvents. The elemental analysis results reveal that Ni(II) complexes have 2:1 stoichiometric ratio of ligand and metal and the data are collected in **Table S1**. Molar conductance of the Ni(II) complexes (10^{-4} mol/L) have been measured at room temperature in CH_3CN and the values of the complexes (**2a-e)** range 14–26 $\Omega^{-1}cm^2mol^{-1}$. The low values infer that the complexes were non-electrolytic nature. Furthermore, the structures of Schiff base ligands (**1a-e**) and Ni(II)-Schiff base complexes (**2a-e**) were established by the following spectral techniques.

The magnetic moment of Ni(II) complexes(**2a-e**) were recorded to assess the geometry. These values were found to be zero for all the examined samples. The results confirm the diamagnetic nature of Ni(II) complexes(**2a-e**) having square planar geometry(**Table S1).**

3.1. Spectral studies

The ^{1}H NMR spectra of the Schiff base ligands (**1a-e**) are recorded at room temperature using DMSO-d_6 as solvent. The sample ^{1}H NMR spectra of ligands are shown in **Figs. S1-S2** and their data are given in **Table S2**. ^{1}H NMR signal for azomethine(-CH=N-) protons of ligands (**1a-e**) are appeared singlet at around 8.26–8.7 δ ppm and another singlet observed around 12.67–13.17 δ ppm corresponding to the phenolic (-OH) protons of the ligands. In the aromatic region, ten protons are observed for ligands (**1a-e**), all aromatic protons appeared as multiplet in the range of 6.5–7.7 δ ppm. The NMR spectrum of ligand (**1d)** showed a singlet at 2.50 δ ppm, which is attributed to methyl group attached to the aromatic ring. The signal at 3.9 δ ppm is assigned to the methoxy group attached to the aromatic rings for the ligand (**1e**).

The data on the important infrared spectral bands of the ligands (**1a-e**) and the metal complexes (**2a-e**) are presented in **Table S3**. FT-IR spectra of ligands (**1a-e**) and Ni(II) complexes(**2a-e**) are shown in **Figs. S3** and **S4**. The IR spectra of Schiff base ligands (**1a-e**) showed a band in the region 3056–3378 cm^{-1}, due to the vibration of phenolic OH group. The characteristic azomethine ν(C=N) stretching frequency band of the ligands (**1a-e)** is lying between 1611 cm^{-1} and 1617 $cm^{-1}$and are shifted to a lower frequency region ranging 1598–1614 cm^{-1} for the Ni(II) complexes (**2a-e)**. The appreciable shifts to the lower frequency for about 10 cm^{-1} for the complexes suggest the involvement of imine nitrogen in coordination with metal ion. For the Ni(II) complexes, a broad band around 3350–3393 cm^{-1} is assigned to stretching vibration of the –OH group of water in coordination sphere. The appearance of two new bands in the spectra of complexes in the range 540–580 cm^{-1} and 440–476 cm^{-1}, indicate the stretching frequency of ν(M-O) and ν(M-N), respectively [44].

The mass spectra of the ligands and the Ni(II) complexes were recorded and the mass values were similar to that of the formula weight and the mass spectra of the ligand **1a** and complex **2a** are shown in **Figs. S5** and **S6, respectively**. The mass spectra of ligands (**1a-e**) show a molecular ion peaks at $m/z = 316$, 385, 474, 344 and 376, which is consistent with the formula weight of the ligands, respectively. The mass spectra of the complexes (**2a-e**) showed molecular ion peaks at m/z = 373, 442, 530, 401 and 433, coinciding with the molecular weight of the complexes, respectively.

Electronic absorption spectra of the Schiff base ligands and Ni(II) complexes were recorded in CH_3CN and the spectra are shown in **Fig. S7**. The absorption spectra of Schiff base ligands (**1a-e**) with λ_{max} values ranging from 269340 nm can be assigned to π-π* transitions of the aromatic rings. The characteristic absorption peaks observed within 327–416 nm region are due to azomethine π-π* and n-π* transitions. The electronic spectra of Ni(II) complexes show absorption peak at around 370–382 nm (MLCT) and 473–505 nm (d-d transition), which suggest square planar geometry of the complexes [45].

The powder X-ray diffractograms of the synthesized compounds were recorded in the range (2theta = 0–80), shown in **Figs. S8** and **S9**. The PXRD patterns of ligands (**1a-e**) showed sharp crystalline peaks indicating their crystalline nature of the free ligands. XRD spectra of Ni(II) complexes (**2a-e**) exhibited less intense and broaden reflections suggesting their amorphous nature. Debye Scherrer's Eq. [46] is used to calculate the average crystallite size of the synthesized compounds and found to be in the range 23–49 nm. From these results, it is identified that the crystallinity of the free ligands decreased upon complexation with Ni(II) ion.

Electrochemical studies of the Ni(II) complexes were carried out by cyclic voltammetry in the potential range of 1.5 to −2 V. The cyclic voltammograms of Ni(II) complexes(**2a-e**) are depicted in **Fig. S10**. In the cyclic voltammogram of each complex, an irreversible wave is observed for the reduction of Ni(II) to the Ni(I). These results revealed that the ligands are electrochemically-inactive in the studied potential range.

3.2. DFT calculations

The geometry optimization was performed, employing Kohn-Sham density functional theory (DFT), as this method is well suited for transition metal containing complexes. Since meta-GGA functional is highly sensitive to grid points, the spin-restricted and spin-unrestricted calculations of Ni(II) complexes are executed using ultrafine grid containing 99 Euler-Maclaurin radial grid points and 590 Lebedev angular grid points and the results are summarized.

3.2.1. Frontier molecular orbitals (FMOs)

From the calculated values, the optimized geometries for Ni(II) complexes (**2a-e**) are found to be planar and the optimized structures are exhibited in Fig. 1.

Frontier molecular orbitals contain quantum chemical parameters such as the Highest Occupied Molecular Orbital (HOMO), Lowest Unoccupied Molecular Orbital (LUMO) and the band gaps (HOMO–LUMO gap) for (**2a-e**) are shown in Fig.2.

It has emerged that the LUMO energies of the complexes (**2a-e**) are comparable ranging from −2.04 eV to −2.55 eV, while the HOMO orbital energy is primarily affected by the Ni(II) metal center. Fig. 2, clearly depicts the energy gap between HOMO and LUMO energy levels. From the energy level results, it is obvious that the complexes **2d (−5.68 eV)** and **2e(−5.46 eV)** with electron donating groups posses higher energy of the HOMO than that of parent complex **2a (−5.87 eV),** while the complexes **2b(−6.06 eV)** and **2c(−6.12 eV)** having electron withdrawing groups have lower energies.

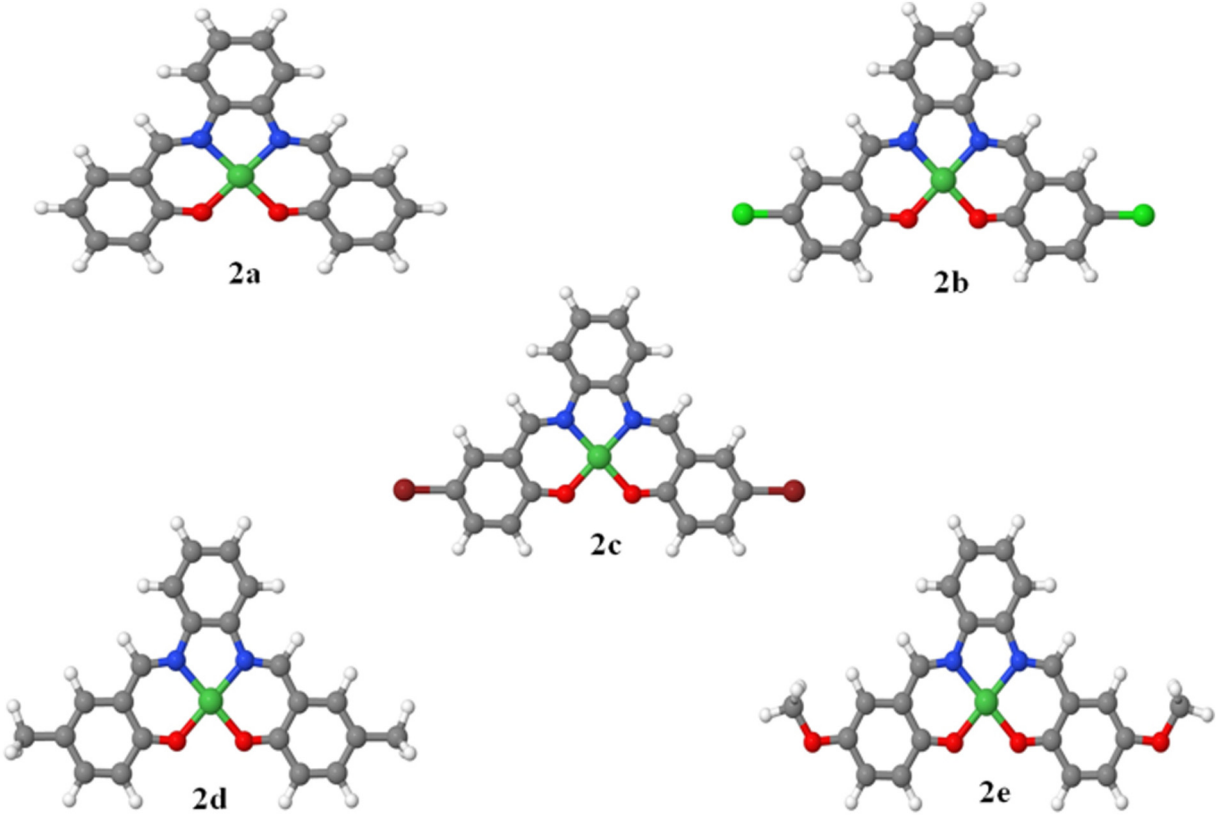

Fig. 1. Optimized geometries of Ni(II) complexes (**2a-e).**

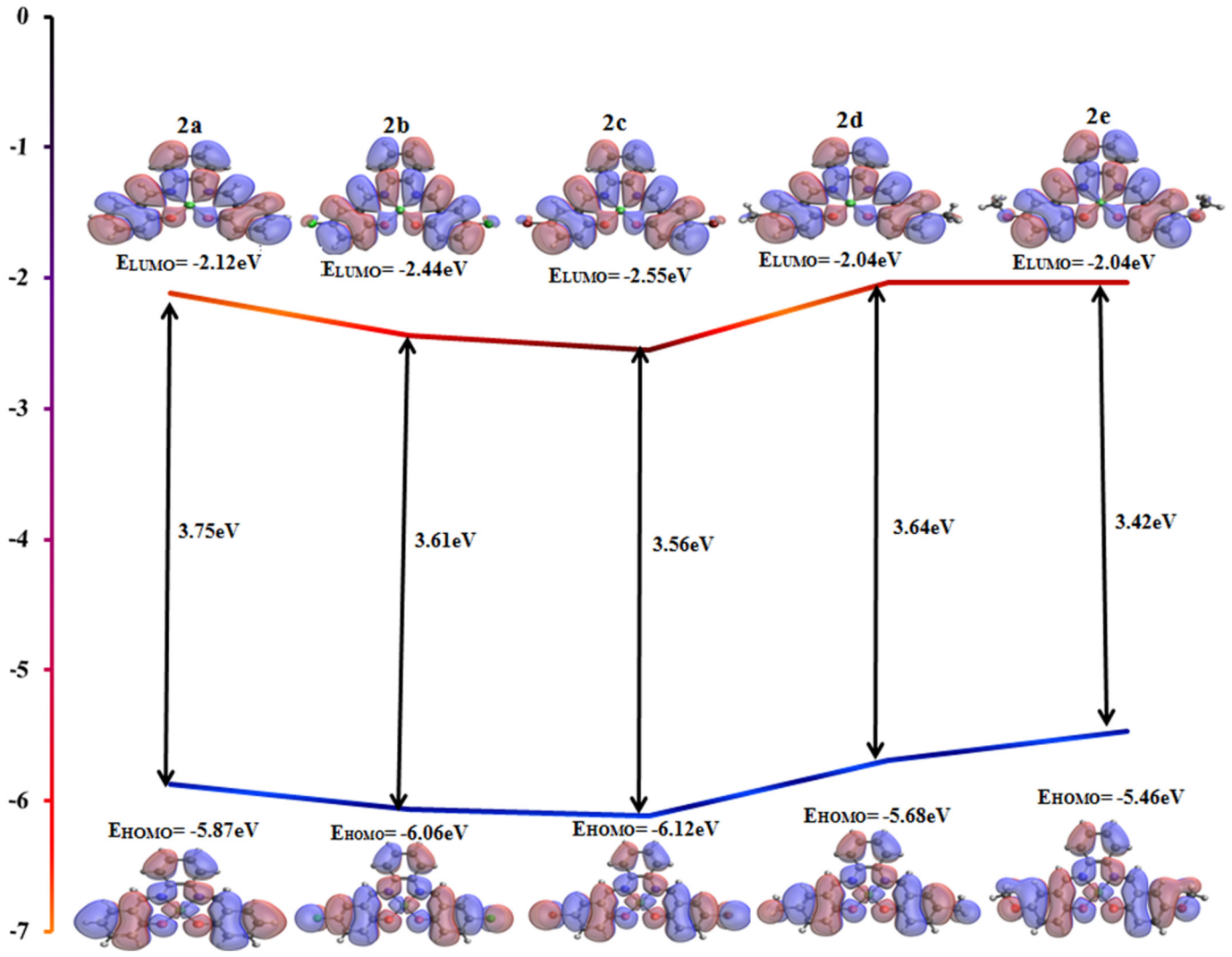

Fig. 2. Frontier molecular orbital diagram of Ni(II) complexes (**2a-e**).

3.2.2. Chemical reactivity descriptors

The global chemical reactivity parameters such as ionization potential (IE), electron affinity (A), electronegativity (χ), chemical hardness (η), chemical softness (S), electrophilicity index (ω) and chemical potential (μ) were able to reveal the reactivity and stability of the complexes [47,48]. Consequently, the chemical reactivity

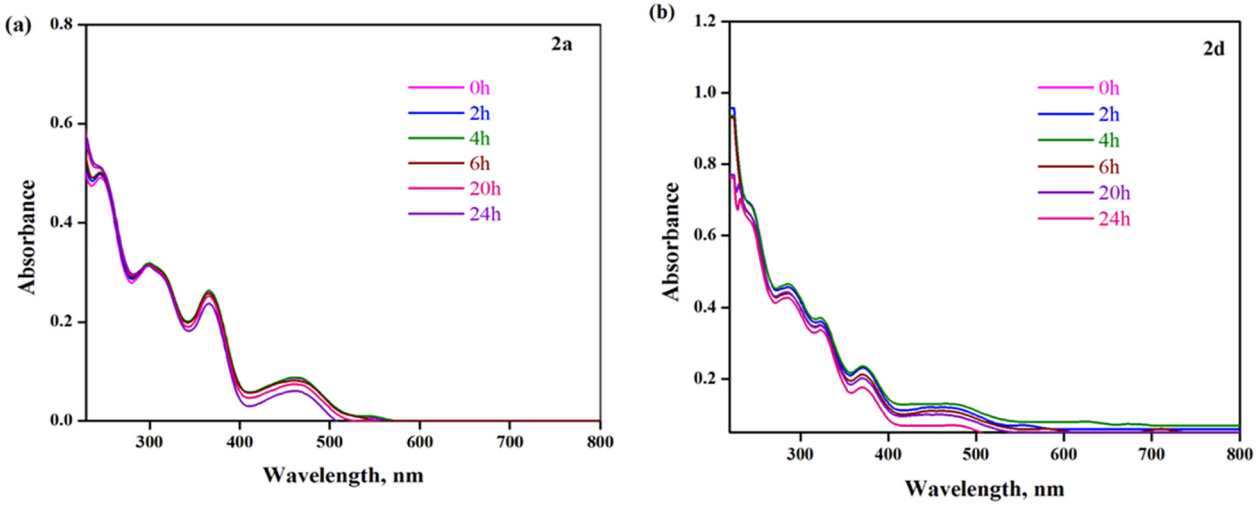

Fig. 3. UV- visible spectra (a) **2a** and (b) **2d** for a period of 24 h.

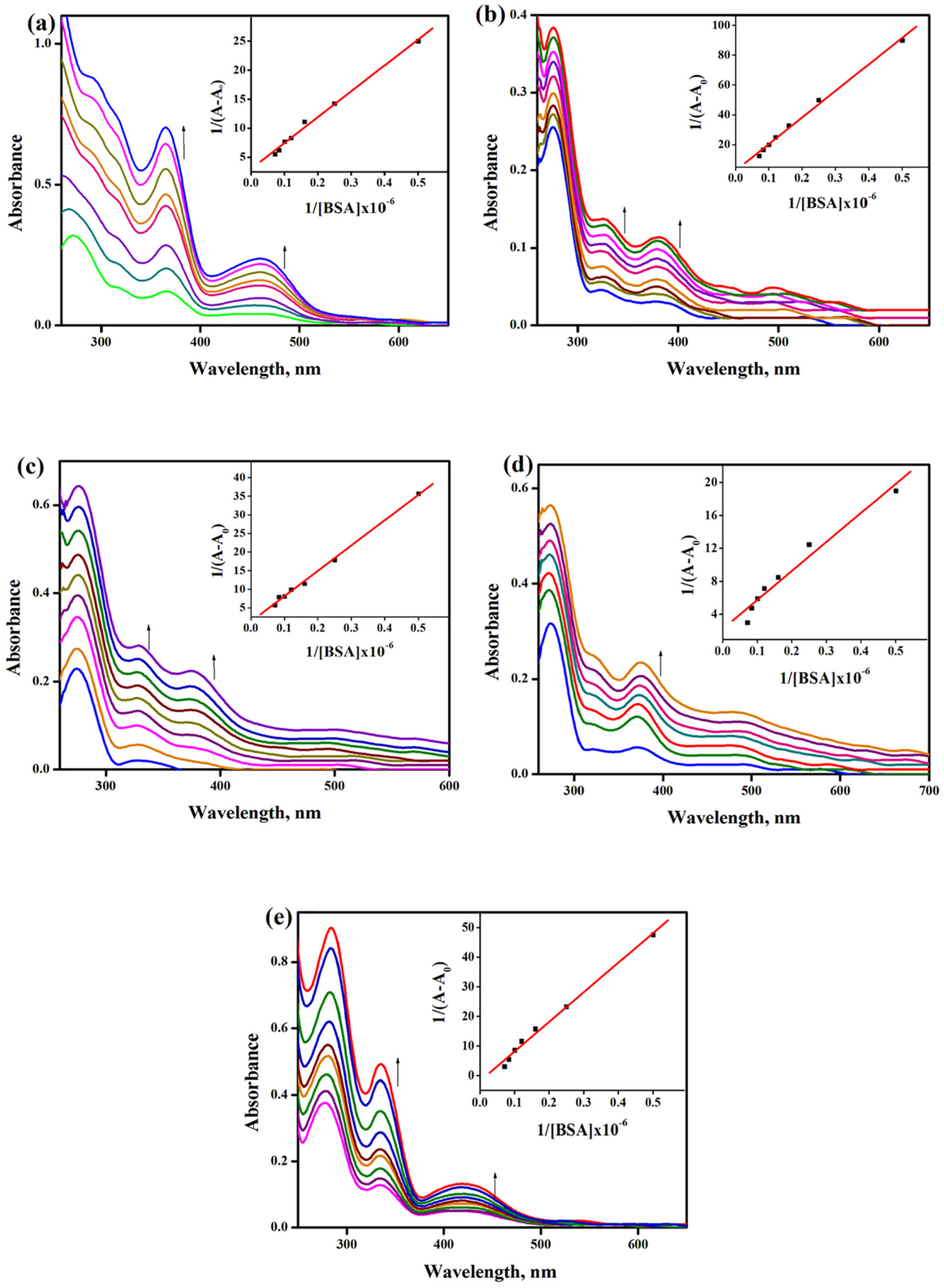

Fig. 4. Absorption spectral changes of Ni(II) complexes **2(a-e)** in the presence of increasing amount of BSA at pH = 7.4. Arrows indicate the absorbance changes upon increasing BSA concentration.

descriptors were ascertained with the help of the energies of frontiers HOMO and LUMO orbitals of the complexes (**2a-e**). The stability and reactivity of any chemical system were represented by chemical hardness, $\eta = (E_{LUMO} - E_{HOMO})/2$. Electronegativity, the power of any atom in a molecule to attract electrons towards it can be obtained by the expression $\chi = -(E_{HOMO} + E_{LUMO})/2$. The negative term of electronegativity of a molecule was defined as the chemical potential, $\mu = (E_{HOMO} + E_{LUMO})/2$. The electrophilic index indicates that the measurement of affinity or capacity of a system to accept electrons was arrived by $\omega = \mu^2/2\eta$.

An overview of the data presented in **Table S4**, the energy gap values for the complexes (**2a-e**) are informative of their chemical reactivity. When the energy gaps between HOMO-LUMO are higher, the complexes become kinetically stable and associated with less chemical reactivity [47,49]. Among the complexes, (**2a-e**) under investigation, the parent unsubstituted complex **2a** seems to have the highest energy gap and is considered to be the hardest molecule, whereas **2e** with very low HOMO-LUMO energy gap is kinetically unstable and favors for the biological binding capability. The decreasing HOMO energies of the complexes lie in the order **2e** > **2d** > **2a** > **2b** > **2c,** indicating their interaction ability with biomolecules in the same order.

The electrophilicity index is a descriptor of chemical reactivity [50]. The present investigation, among the complexes the electrophilicity index values for **2d** and **2e** may be due to stabilization of energy of the system through additional electronic charges from electron donating (-CH_3 and –OCH_3) environment in the phenyl ring. This reflects in the biological activities of these complexes (**2d** and **2e**) having higher binding nature than the other complexes (**2a**, **2b** and **2c**).

3.3. Solution stability of the complexes

Stability of a complex in a buffer solution is a fundamental property in the development of potential anticancer drugs. The stability study is evaluated using UV–visible absorption spectroscopy in different times within 24 h at 37 °C. It is possible to qualitatively determine the stability of the complexes under physiological conditions, by dissolving them in Tris-buffer at pH 7.4. The results of the stability of the Ni(II) complexes are depicted in Fig.3.

All the Ni(II) complexes exhibit a strong absorption bands in the range 370-382 nm, which can be assigned to MLCT. Besides a broad and weak absorption band between 462 nm and 492 nm, attributes to d-d transitions. In all the complexes, the positions of the peaks of the complexes are maintained unchanged within the determined time and the decrease in band intensity does not affect the general stability of the complexes [51]. Consequently the results reveal that the complexes (**2a-e**) are stable under physiological conditions.

3.4. BSA binding studies.

3.4.1. Electronic absorption spectral titration

All the five Ni(II) complexes **2a-e** show an enhancement in its MLCT absorption on the addition of BSA. The absorption spectral changes of the Ni(II) complexes (**2a-e**) on the addition of BSA are depicted in Fig.4. The characteristic absorption peak for [BSA] = 2 μM at 280 nm, corresponds to tryptophan (Trp) and tyrosine (Tyr) residues in proteins [52]. The absorption intensity of complex **2a** (2 μM) at 365(0.12) and 460 nm (0.04), in the experimental condition, increase obviously upon successive addition of [BSA] = 0–18 μM. It is important to note that the absorption intensity of Ni(II) complex **2a** at 365 and 460 nm enhanced upto 0.70 and 0.23 respectively, which may be due to non-covalent type of interaction between complex **2a** and BSA.

Similar observations are made for complexes (**2b-e**). This result is taken as the first spectral information towards the binding of **2a** with BSA. Form the spectral data, the binding constants (K) for the interaction of ligands (**1a-e**) as well as complexes (**2a-e**) with BSA are calculated using Benesi-Hildebrand eq. (1) [53].

$$\frac{A_0}{A-A_0} = \left(\frac{\varepsilon_{BSA}}{\varepsilon_C}\right) + \left(\frac{\varepsilon_{BSA}}{\varepsilon_C}.K\right) \times \frac{1}{[BSA]} \quad (1)$$

Here, A_0 and A are the absorbance of complexes in the absence and presence of BSA, ε_{BSA} and ε_C are the molar extinction coefficients of the BSA bound and free ligand/Ni(II) complex. A linear reciprocal plot is obtained by plotting $1/(A\text{-}A_0)$ vs 1/[BSA]. The binding constants (K) for the interaction of BSA with ligands and Ni(II) complexes are calculated from the ratio of the intercept to the slope. Benesi-Hildebrand plot is shown in insets Fig.4. The binding constant values for interaction of ligands and Ni(II) complexes with BSA are tabulated in Table 1.

From the results in Table 1, it is inferred that the binding constant values, K, of the Ni(II) complexes (**2a-e**) are higher than their corresponding ligands (**1a-e**). The results suggest that the Ni(II) complexes interact more strongly with BSA, which is probably attributable to the potential synergistic effect when their ligands are coordinated to the nickel metal ion [54]. The molecular diversity is also identified by the results of complexes **2d** and **2e** with electron-donating group which possess higher binding constant values than the parent complex **2a**, whereas the complexes **2b** and **2c** with electron withdrawing groups have lower binding constant values than the parent complex **2a**.

3.4.2. Fluorescence quenching of BSA by Ni(II) complexes

In order to learn the interaction of the synthesized Ni(II) complexes with BSA, the fluorescence quenching studies are carried out. The results show that the fluorescence intensity of BSA is decreased significantly on adding complexes with a red shift from 335 to 340 nm. The fluorescence spectral changes of BSA are depicted in Fig.5.

These fluorescence spectral changes imply that the Ni(II) complexes bind strongly with BSA. On increasing the concentration of the complex, apart from the fluorescence quenching of BSA at 340 nm, a notable observation is made that the luminescence band corresponding to the complex **2a** is regenerated at 450 nm. The intensity of this band increases with an increase in the concentration of the quencher. An isosbestic point observed at 398 nm is also an indicative of BSA interaction with the complex **2a**. Similar behavioral changes with clear isosbestic points are observed for all the complexes (**2b-e**) with hypsochromic shift ranging from 10 to 49 nm, revealing a definite interaction of the complexes with BSA protein. The fluorescence quenching is examined by the Stern-Volmer eq. (2)

$$F_0/F = 1 + K_{SV}[Q] = 1 + K_q\tau_0[Q] \quad (2)$$

where F_0 and F are the fluorescence intensities of fluorophore in the absence and presence of the quencher, [Q] is the quencher concentration, k_q is the biomolecular quenching constant and $\tau_0$is the average lifetime of protein without quencher (about 10^{-8} s). K_{SV} is the Stern-Volmer quenching constant and is calculated from a plot of F_0 /F vs [Q] (insets in Fig.5).

The equilibrium between free and bound molecule for the binding of small molecules independently to a set of equivalent sites on a macromolecule, are demonstrated according to the Scatchard eq. (3) [55(a)].

$$\log(F_0\text{–}F)/F = \log K_b + n \log[Q] \quad (3)$$

where K_b is the binding constant of the complex with BSA and n is the number of binding sites. The values of K_b and n are calculated from

Table 1
Binding constant for ligands (**1a-e**) and Ni(II) complexes (**2a-e**) with BSA.

Ligand	K(M^{-1})	Complex	K(M^{-1})
1a	2.4×10^3	**2a**	5.1×10^4
1b	1.6×10^3	**2b**	1.9×10^4
1c	1.3×10^3	**2c**	2.1×10^4
1d	3.6×10^3	**2d**	5.4×10^4
1e	4.2×10^3	**2e**	5.8×10^4

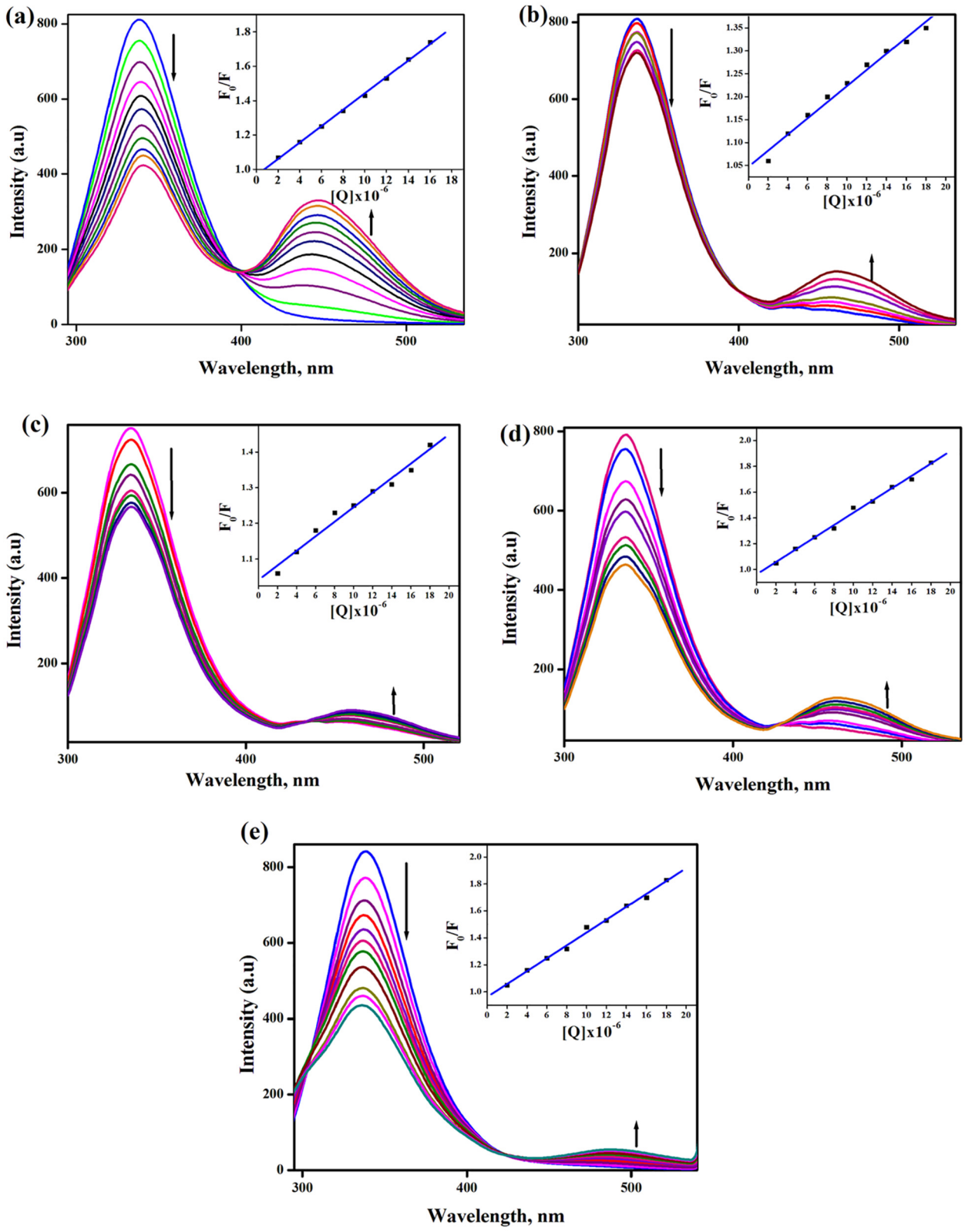

Fig. 5. Fluorescence spectra of BSA with the addition of Ni(II) complexes **2 (a-e)** at pH = 7.4. Arrows indicates the changes in intensity.

the intercept and slope of a plot of log [(F_0–F)/F] vs log[Q] as shown in **Fig.S11**. The K_{SV}, k_q, K_b and n values of synthesized Ni(II) complexes are depicted in Table 2.

The observed values are indicative of the binding capability of the complexes with BSA in the order complex **2e** > complex **2d** > complex **2a** > complex **2b** > complex **2c**. The K_b value is used to evaluate the strength of the binding nature. The K_b value for the complex **2e** is 5.9×10^4 which suggested the good binding affinity than other complexes (**2a-d**). From the results it is clear that the Ni(II) complexes have only one binding site available to interact with BSA protein.

Table 2
Quenching constant, binding constant and number of binding sites for interactions of Ni (II) complexes (**2a-e)** with BSA.

Complex	K_{SV} (M^{-1})	k_q(M^{-1} s^{-1})	K_b (M^{-1})	n
2a	5.1×10^4	5.1×10^{12}	5.8×10^4	1.00
2b	3.6×10^4	3.6×10^{12}	3.4×10^4	0.97
2c	2.9×10^4	2.9×10^{12}	2.7×10^4	0.95
2d	5.7×10^4	5.7×10^{12}	5.4×10^4	0.99
2e	6.1×10^4	6.1×10^{12}	5.9×10^4	1.01

The binding constant values (K_a) were also determined from Hill's plot using the eq. (4)

$$\log(\theta/(1-\theta)) = n\ \log[Q] + \log Ka \quad (4)$$

where, θ is the fractional occupancy, n, number of binding sites and K_a is the association constant. The plots drawn between log[θ/(1- θ)] versus log[Q] are linear(**Fig.S12**). The values of **n** and $\mathbf{K_a}$ for the binding of Ni (II) complexes with BSA are acquired from the slope and intercept, respectively and the data are depicted in **Table S5.** The observed results show that the n values are greater than $1(n > 1)$ which predicts the positive cooperative binding [55(b)].

3.4.3. Electrochemical studies

As an additional technique to study the binding of the Ni(II) complexes (**2a-e)** with BSA, cyclic voltammetric measurements were studied both in the presence and absence of BSA. A typical electrochemical behavior of complexes in the presence and absence of BSA is shown in Fig. 6. The cyclic voltammetric data of complex **2a** show one irreversible wave due to the reduction of Ni(II) to the Ni(I) form at a cathodic peak potential, E_{pc} − 0.937 and cathodic peak current, i_{pc} 2.677×10^{-5}A for complex **2a**. On addition of BSA, the peak current of complex **2a** decreased significantly and the peak potential shifts towards lower potential region −0.740 V. Similar observations are made for complexes (**2b-e**). The shift in the peak potential can be inferred to electrostatic interaction of the complex with protein [56]. It is suggested that Ni(II) complexes form an electrochemically non-active complex with BSA. The decrease in the peak current at higher concentrations of BSA is attributed to the formation of Ni(II) complex-protein adduct.

The change in the peak current of complexes (**2a-e**) by the addition of varying concentration of BSA is used to calculate the binding constant using the eq. (5) [57].

$$\log(1/[BSA]) = \log K + \log\left(\frac{I}{I_0} - I\right) \quad (5)$$

Here K is the binding constant, I_0 and I are the peak currents of the free and BSA bound complex, respectively. From the linear plot shown in **Fig. S13**, log (1/[BSA]) vs $\log(I/(I_0–I))$ the binding constant is obtained and the values are in the range 0.8–4.6×10^4 M^{-1}. Binding constant values acquired by the cyclic voltammetric technique are similar to the values determined from the absorption and emission spectral studies providing strong support for binding of BSA with Ni(II) complexes (**2a-e).**

3.5. Molecular modeling for the binding of Ni(II) complexes with BSA

Molecular docking is an attractive scaffold to understand drug-biomolecule interactions for the rational drug design. In the present study, molecular docking is used to investigate the binding energy and binding site of complexes (**2a-e)** with BSA. The representative docked structures are shown in Fig.7.

These structures are used to study various intermolecular interactions and to determine the relative binding energy of the docked complexes, which are depicted in Table 3.

The results of docking studies reveal that all the synthesized molecules showed binding energy ranging from −6.52 to −8.05 kcal mol^{-1} towards the target BSA protein. The free energy of binding ΔG^0, is based on empirically derived terms which represent common contributions such as the hydrophobic effect, hydrogen bonding and conformational entropy. The affinity can be quantified [58] using the binding free energy, ΔG^0 related to the affinity or binding constant K as

$$\Delta G^0 = -RT\ln K$$

where R is the gas constant and T is the temperature in Kelvin. A negative free energy (Table 3) indicates favorable interaction of the Ni(II) complexes (**2a-e)** with BSA. It is noted that upon comparing the binding energies of different Ni(II) complexes, complex **2e** with BSA has highest binding capability. This study on the interaction of Ni(II) complexes with BSA helps to understand how the drug molecule may affect the structure of proteins when drugs are introduced to target specific diseases.

3.6. Antimicrobial assay

The optimistic results acquired from the antimicrobial studies of the Ni(II) complexes (**2a-e)** are found to be potentially active in comparison with their corresponding ligands and metal salt against strains of bacteria and fungi used. This infers that the activities of ligands are enhanced on complexation, which can be explained on the basis of the theory of chelation [59]. The screening results are shown in Fig.8 and zone of inhibition values of metal salt, Schiff base ligands (**1a-e**) and Ni(II) complexes (**2a-e)** are tabulated in **Table S6**.

The results obtained for screening of the $NiCl_2.6H_2O$, free ligands and synthesized Ni(II)-Schiff base complexes against bacteria and fungi are shown in **Table S6.** The Ni(II)-Schiff base complexes have higher antimicrobial activities compared to $NiCl_2.6H_2O$ against the tested microorganisms under identical experimental conditions. The observed remarkable activity of complexes **2d** and **2e** against bacteria and fungi are found to be almost close to that of the control drug. This may be due to the effect of electron donating groups present in the aromatic moiety. Complexes **2b** and **2c** showed lower activity against *S. aureus* and *A. Niger* compared to other complexes, which may be due to the presence of electron withdrawing groups. Moreover, it is inferred that the metal complexes are more effective than the ligands. This may be due to the fact that the ligand is activated by the metal ion on complexation.

3.7. Cytotoxicity assay

The in vitro cytotoxicities of Schiff base ligands (**1a-e)** and Ni(II) complexes (**2a-e)** were evaluated at different concentrations (20–140 μM/) against human breast cancer(MCF-7) cell lines using MTT assay. The results are analyzed by means of cell inhibition expressed as cell viability of the complexes relative to the control. The histograms of the cell viability assay for Ni(II) complexes (**2a-e)** against MCF-7 cells and the cell images are illustrated in Fig.9 **(**i) and (ii) respectively. IC_{50} values of ligands (**1a-e)** and Ni(II) complexes (**2a-e)** towards MCF-7cell lines are provided in Table 4.

As can be seen from the results, ligands exhibited cytotoxicity with IC_{50} values ranging from 61.3–82.1 μM against MCF-7 cell lines. However the inhibitory nature remarkably increased for the Ni(II) complexes with IC_{50} values ranging from 5.4–29.1 μM. The results suggest that Ni(II) complexes (**2a-e)** show more significant anticancer activity than their corresponding ligands (**1a-e)** against MCF-7cell lines. On analyzing the anticancer activity of the complexes (**2a-e)**, electron donating groups bearing complexes **2d** and **2e** demonstrate lower cytotoxcity than the parent complex **2a**, on the other hand the complexes **2b** and **2c**

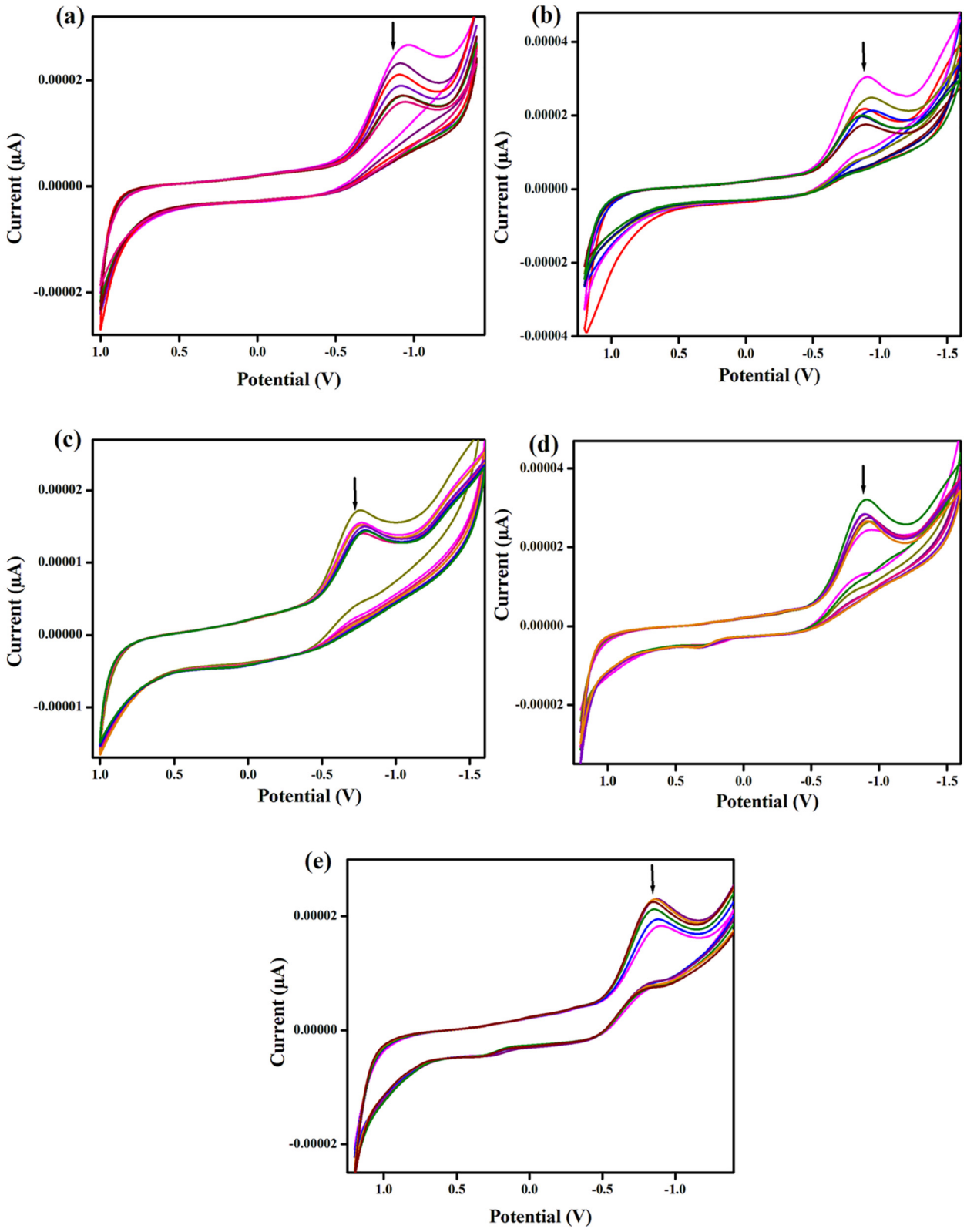

Fig. 6. Cyclic voltammetric diagram of Ni(II) complexes **2(a-e)** in the presence and absence of BSA.

with electron withdrawing groups have higher activity than the parent complex **2a**.

The observed results for the IC_{50} values of complexes **2d** and **2e** tempted us to report that the electronic environment might be one of the important factors for the anticancer activity. This gives insight for designing of anticancer drugs with improved efficiency.

*3.8. Cell images before and after treatment with complex **2e***

The IC_{50} value of complexes **2d** (8.6 µM) and **2e** (5.4 µM) is compared with the results obtained by the authors [17] for cisplatin (23.70 µM) against MCF-7 cell line. It is interesting to note that the complexes **2d** and **2e** showed excellent activity in breast cancer (MCF-7) cell

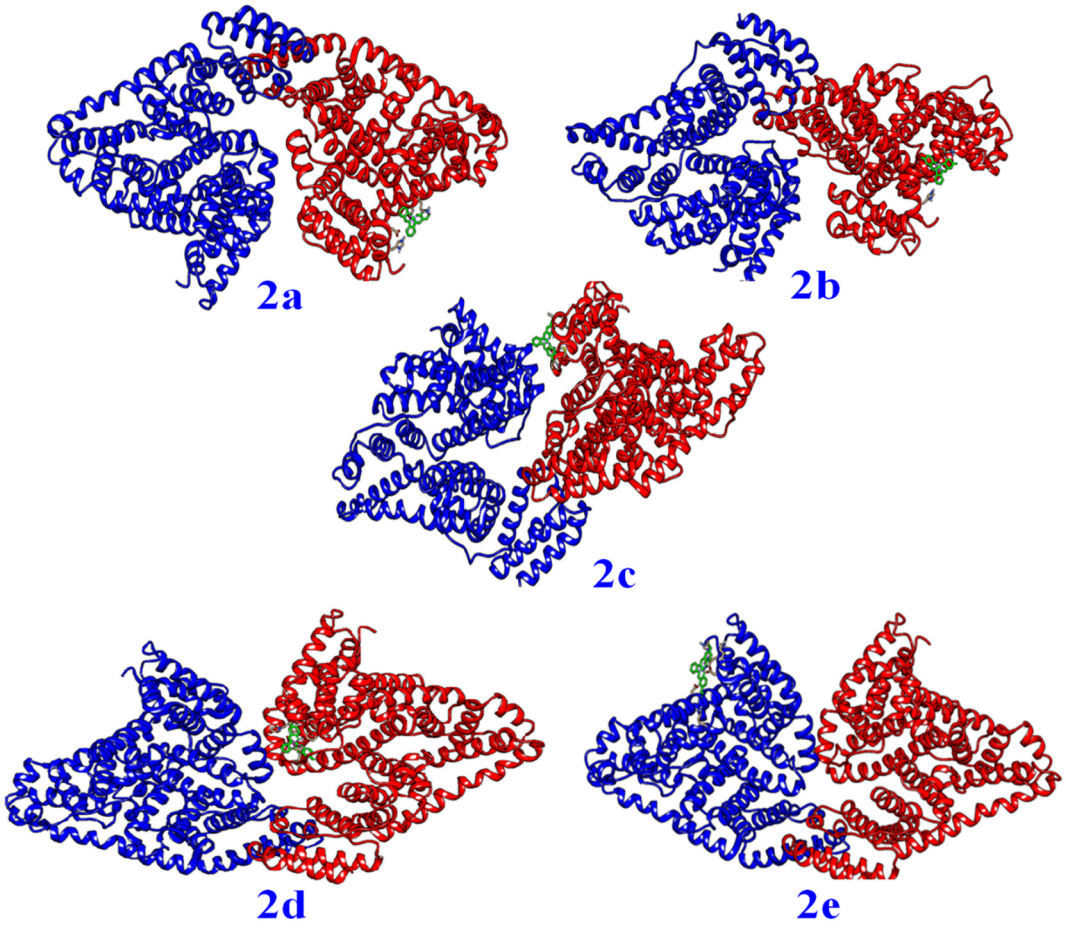

Fig. 7. Molecular docking poses of Ni(II) complexes (**2a-e)** with BSA.

Table 3
Docking studies results of Ni(II) complexes (**2a-e)** with BSA.

Complex	Binding energy (kcal mol^{-1})	Ligand efficiency (kcal mol^{-1})	Inhibitory constant	Intermolecular energy (kcal mol^{-1})	Vdw desolvation energy (kcal mol^{-1})	Electrostatic energy (kcal mol^{-1})
2a	−7.23	−0.28	3.00	−7.53	−5.08	−0.46
2b	−8.05	−0.30	1.26	−8.05	−7.15	−0.89
2c	−7.26	−0.29	4.74	−7.26	−3.78	−3.48
2d	−7.19	−0.27	5.41	−7.19	−3.71	−3.48
2e	−6.52	−0.22	6.72	−7.41	−3.88	−3.53

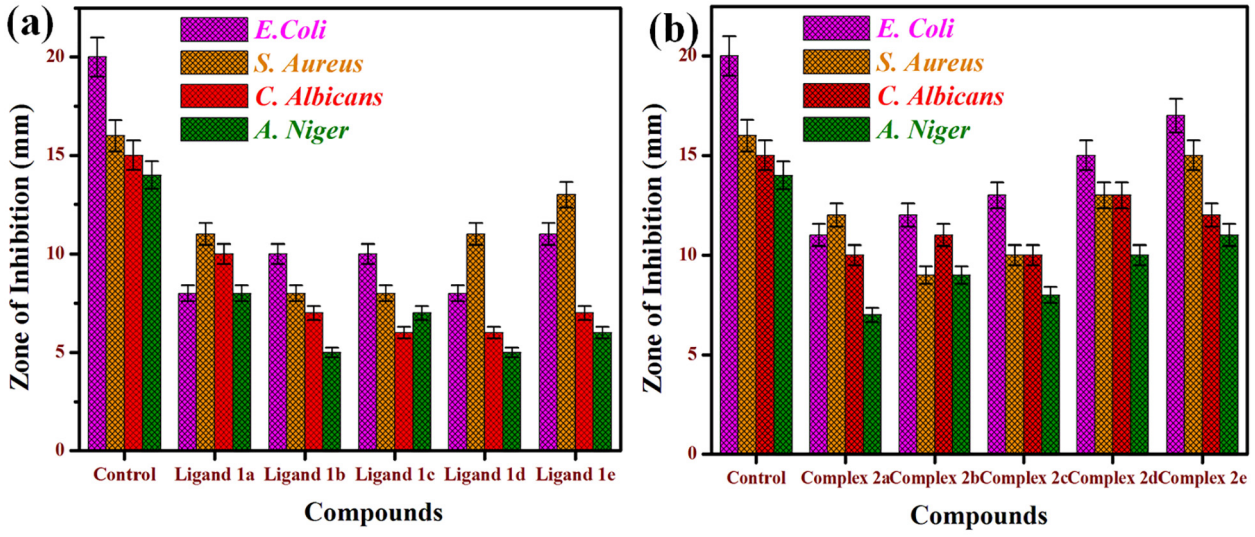

Fig. 8. Antimicrobial activity of (a) ligands (**1a-e**) and (b) Ni(II) complexes (**2a-e).**

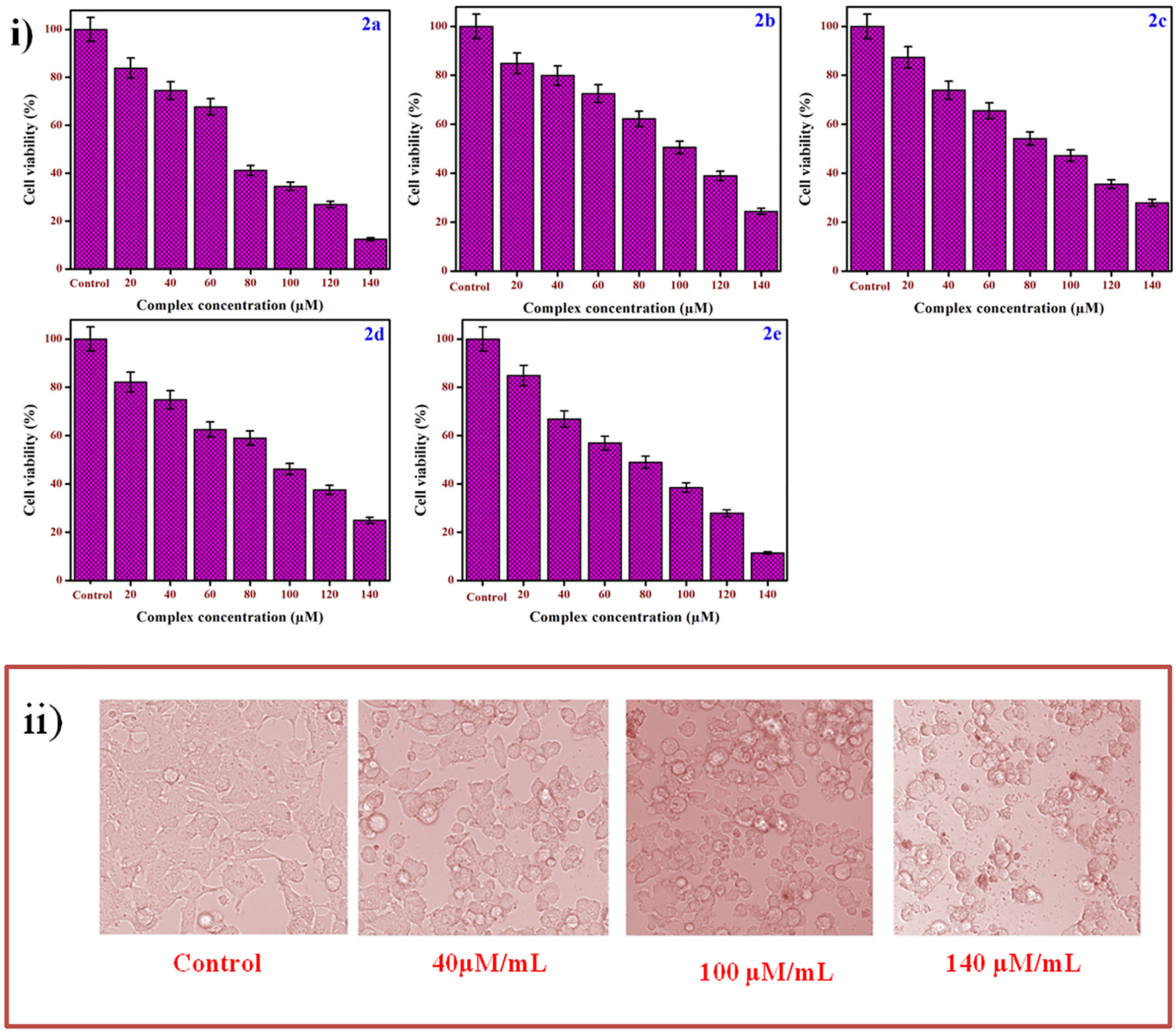

Fig. 9. (i) Cell viability of complexes (**2a-e)** on MCF-7 cell lines.

line. The superior activity of the complexes **2d** and **2e** assumes significance due to the presence of electron donating substituents. Ni(II) complex **2e** showed almost four fold higher activity when compared with cisplatin against MCF-7 cell line.

It is also worth to compare the results observed with V(IV)-salphen complexes towards the AGS gastric cell lines by Gomathi et.al [29].. Our previous report shows that the V(IV)-salphen complexes exhibit broad inhibition on the AGS gastric cell lines with IC_{50} values in the range 0.4–38.9 μM. From the present study we realize that Ni(II)-Schiff base complexes (2a-e) have IC_{50} values in the range 5.4–29.1 μM. On viewing the same environment of both the studies, the inhibitory effects of Ni(II) complexes bearing electron donating and electron withdrawing groups have comparable anticancer activity towards cancer cell lines. Further comparison of behavior of Ni(II)-salphen complexes with the Zn (II)-salphen complexes employed by Giannicchi et.al [27]. shows that Zn (II)-salphen complexes have higher IC_{50} values ranging from 71 to 1073 μM compared to the Ni(II)-salphen complexes. Thus it is appropriate to state that Ni(II)-salphen complexes have better cytotoxic activity compared with Zn (II)-salphen complexes and comparable activity with V(IV)-salphen complexes.

Table 4
IC_{50} values of ligands (**1a-e)** and Ni(II) complexes (**2a-e)** towards MCF-7cell lines.

Ligands	IC_{50} (μM)	Ni(*II*)complexes	IC_{50} (μM)
1a	70.3 ± 3.51	**2a**	26.1 ± 1.30
1b	75.5 ± 3.77	**2b**	29.1 ± 1.45
1c	82.1 ± 4.10	**2c**	28.4 ± 1.42
1d	61.3 ± 3.06	**2d**	8.6 ± 0.43
1e	69.4 ± 3.47	**2e**	5.4 ± 0.27

4. Conclusion

The present investigation focuses on the syntheses of a series of Ni (II) complexes (**2a-e)** from N_2O_2 donor carrying Schiff base ligands (**1a-e)**. Spectroscopic characterization (^{1}H NMR, FT-IR, Mass, UV–vis

and PXRD) supported the formation of the complexes. Spectral results and magnetic moments data suggest that complexes (**2a-e)** have square planar geometry around the central metal atom. The molar conductivity measurements indicated that all Ni(II) complexes (**2a-e)** are non electrolytes. DFT simulations reveal that the optimized geometries for complexes (**2a-e)** were found to be planar. The study of BSA binding efficiency of ligands and Ni(II) complexes by absorption, emission and cyclic voltammetry methods support the strong interaction of Ni(II) complexes with BSA. Molecular docking studies suggest that Ni(II) complexes(**2a-e)** have better binding affinity towards BSA. All these results of BSA binding studies revealed that the complexes **2d** and **2e** have greater binding ability among the chosen complexes. The results of antimicrobial activity demonstrate that the Ni(II) complexes have better activity than that of corresponding ligands as well as the precursor, under identical experimental conditions. The in vitro anticancer activity of ligands and Ni(II) complexes were evaluated against MCF-7 cell line and compared with the published results obtained for cisplatin, the well-known antitumour agent and V(IV)-salphen and Zn(II)-salphen complexes. Among all, **2d** and **2e** showed excellent anticancer activity superior to other metal complexes. In particular, complex **2e** exhibited highest activity against MCF-7cell line. With the potential results, we conclude that Ni(II) complexes show promising results applicable in the field of anticancer drug designing.

Declaration of Competing Intrest

The authors declare that they have no known competing financial interests or personal relationships that could have appeared to influence the work reported in this paper

Declaration of Competing Interest

None.

Acknowledgements

A.M.I. Jayaseeli gratefully acknowledge the financial support provided by University Grants Commission, New Delhi, India (F.No.43-412/2014(SR)). A.M.I. Jayaseeli and J. Jeevitha Rani extend their sincere thanks to the Management, Jayaraj Annapackiam College for Women, Periyakulam,TN, India for providing research facilities necessary for the execution of this work at Basic Scientific Research (BSR) Laboratory.

Appendix A. Supplementary data

Supplementary data to this article can be found online at https://doi.org/10.1016/j.molliq.2021.115457.

References

[1] Y. Li, Z. Yang, M. Zhou, Y. Li, J. He, X. Wang, Z. Lin, Ni(II) and Co(II) complexes of an asymmetrical aroylhydrazone: synthesis, molecular structures, DNA binding, protein interaction, radical scavenging and cytotoxic activity, RSC Adv. 7 (2017) 41527–41539, https://doi.org/10.1039/C7RA05504H.

[2] P. Kalaivani, S. Saranya, P. Poornima, R. Prabhakaran, F. Dallemer, V. Vijaya Padma, K. Natarajan, Biological evaluation of new nickel(II) metallates: synthesis, DNA / protein binding and mitochondrial mediated apoptosis in human lung cancer cells (A549) via ROS hypergeneration and depletion of cellular antioxidant pool, Eur. J. Med. Chem. 82 (2014) 584–599https://doi.org/10.1016/j.ejmech.2014.05.075.

[3] R.J. Browning, P.J.T. Reardon, M. Parhizkar, R.B. Pedley, M. Edirisinghe, J.C. Knowles, E. Stride, Drug delivery strategies for platinum-based chemotherapy, ACS Nano 11 (2017) 8560–8578 https://doi.org/acsnano.7b04092.

[4] J. Zhao, S. Zhi, H. Yu, J. Zhang, J. Zhang, J. Hu, Synthesis, crystal structure, DNA/BSA interaction and in vitro antitumor activity of N-heterocycle cu(II) and co(II) complexes, J. Coord. Chem. 70 (2017) 3110–3131, https://doi.org/10.1080/00958972.2017.1372573.

[5] G. Facchetti, I. Rimoldi, Anticancer platinum(II) complexes bearing N-heterocycle rings, Bioorg.Med. Chem. Let. 29 (2019) 1257–1263, https://doi.org/10.1016/j.bmcl.2019.03.045.

[6] X. Wang, X. Wang, Z. Guo, Functionalization of platinum complexes for biomedical applications, Acc. Chem. Res. 48 (2015) 2622–2631, https://doi.org/10.1021/acs.accounts.5b00203.

[7] W. Liu, R. Gust, Metal N-heterocyclic carbene complexes as potential antitumor metallodrugs, Chem. Soc. Rev. 42 (2013) 755–773, https://doi.org/10.1039/c2cs35314h.

[8] M. Alagesan, N.S.P. Bhuvanesh, N. Dharmaraj, Binuclear copper complexes: synthesis, X-ray structure and interaction study with nucleotide/protein by in vitro biochemical and electrochemical analysis, Eur. J. Med. Chem. 78 (2014) 281–293, https://doi.org/10.1016/j.ejmech.2014.03.043.

[9] H.J. Kruger, R.H. Holm, Stabilization of trivalent nickel in tetragonal NiS_4N_2 and NiN_6 environments: synthesis, structures, redox potentials and observations related to [NiFe]-hydrogenases, J. Am. Chem. Soc. 112 (1990) 2955–2963, https://doi.org/10.1021/ja00164a018.

[10] Z. Lu, C. White, A.L. Rheingold, R.H. Crabtree, Deprotonated thioamides as thiolate S-donor ligands with a high tendency to avoid M-S-M bridge formation: crystal and molecular structure of bis(2-hydroxy-5- methylacetophenone N,N-dimethylthiosemicarbazonato)dinickel, Inorg. Chem. 32 (1993) 3991–3994, https://doi.org/10.1021/ic00071a006.

[11] G.J. Colpas, M. Kumar, R.O. Day, M.J. Maroney, Structural investigations of nickel complexes with nitrogen and sulfur donor ligands, Inorg. Chem. 29 (1990) 4779–4788, https://doi.org/10.1021/ic00348a037.

[12] S.B. Choudhury, D. Ray, A. Chakravorty, Nickel(III)-sulfur binding. Chemistry of the tris(xanthate) family, Inorg.Chem. 29 (1990) 4603–4611, https://doi.org/10.1021/ic00348a006.

[13] S.W. Ragsdale, H.G. Wood, J.A. Morton, L.G. Ljungdahl, D.V. Dervartanian, The bioinorganic chemistry of nickel, VCH, New York, 1988 Chapter 14.

[14] A. Buschini, S. Pinelli, C.F. Giordani, M.B. Ferrari, F. Bisceglie, M. Giannetto, G. Pelosi, P. Tarasconi, Synthesis, characterization and deepening in the comprehension of the biological action mechanisms of a new nickel complex with antiproliferative activity, J.Inorg. Biochem. 103 (2009) 666–677, https://doi.org/10.1016/j.jinorgbio.2008.12.016.

[15] P. Zhao, S. Zhai, J. Dong, L. Gao, X. Liu, L. Wang, J. Kong, L. Li, Synthesis, structure, DNA interaction, and SOD activity of three nickel(II) complexes containing L-phenylalanine Schiff Base and 1,10-Phenanthroline Bioinorg, Chem. Appl. 2018 (2018) 1–16, https://doi.org/10.1155/2018/8478152.

[16] Z. Abbasi, M. Salehi, M. Kubicki, A. Khaleghian, New Ni(II) complexes involving symmetrical bidentate N,O-donor Schiff base ligands: synthesis at ambient temperature, crystal structures, electrochemical study, antioxidant and cytotoxic activities, J. Coord. Chem. 70 (2017) 3132–3146, https://doi.org/10.1080/00958972.2017.1373189.

[17] G. Kalaiarasi, R. Jain, H. Puschman, S. Poorna Chandrika, K. Preethi, R. Prabhakaran, New Binuclear Ni(II) metallates containing ONS chelators: synthesis, characterisation, DNA binding, DNA cleavage, protein binding, antioxidant activity, antimicrobial and in vitro cytotoxicity, New J. Chem. 41 (2017) 2543–2560, https://doi.org/10.1039/c6nj03516g.

[18] M. Sedighipoor, A.H. Kianfar, W.A.K. Mahmood, M.H. Azarian, Synthesis and electronic structure of novel Schiff bases Ni/cu (II) complexes: evaluation of DNA/serum protein binding by spectroscopic studies, Polyhedron 129 (2017) 1–8, https://doi.org/10.1016/j.poly.2017.03.027.

[19] S. Poornima, K. Gunasekaran, M. Kandaswamy, Nuclease activity and interaction studies of unsymmetrical binuclear Ni(II) complexes with CT-DNA and BSA Dalton Trans, 44, 2015 16361–16371, https://doi.org/10.1039/c4dt01744g.

[20] Y. Li, Y. Li, N. Wang, D. Lin, X. Liu, Y. Yang, Q. Gao, Synthesis, DNA/BSA binding studies and in vitro biological assay of nickel(II) complexes incorporating tridentate aroylhydrazone and triphenylphosphine ligands, J. Biomol. Struct. Dyn. 27 (2019) 1–32, https://doi.org/10.1080/07391102.2019.1694995.

[21] N. Biswas, S. Khanra, A. Sarkar, S. Bhattacharjee, D.P. Mandal, A. Chaudhuri, S. Chakraborty, C.R. Choudhury, Cytotoxicity activity, in silico molecular docking, protein- and DNA-binding study of a new Ni(II) Schiff base complex J, Coord. Chem. 71 (2018) 2740–2766, https://doi.org/10.1080/00958972.2018.1492118.

[22] O.M.I. Adly, M. Shebl, E.M. Abdelrhman, B.A. El-Shetary, Synthesis, spectroscopic, X-ray diffraction, antimicrobial and antitumor studies of Ni(II) and co(II) complexes derived from 4-acetyl-5,6-diphenyl-3(2H)-pyridazinone and ethylenediamine, J. Mol. Struct. 1219 (2020) 128607–128618, https://doi.org/10.1016/j.molstruc.2020.128607.

[23] V.K. Sivasubramanian, M. Ganesan, S. Rajagopal, R. Ramaraj, Iron(III)-Salen complexes as enzyme models: mechanistic study of Oxo(salen)iron complexes oxygenation of organic sulfides, J. Org. Chem. 67 (2002) 1506–1514, https://doi.org/10.1021/jo010878o.

[24] A.M.I. Jayaseeli, S. Rajagopal, [Iron(III)–salen] ion catalyzed H_2O_2 oxidation of organic sulfides and sulfoxides, J. Mol. Catal. A: Chem. 309 (2009) 103–110, https://doi.org/10.1016/j.molcata.2009.05.004.

[25] M.S. More, S.B. Pawal, S.R. Lolage, S.S. Chavan, Syntheses, structural characterization, luminescence and optical studies of Ni(II) and Zn(II) complexes containing salophen ligand, J. Mol. Struct. 1128 (2017) 419–427, https://doi.org/10.1016/j.molstruc.2016.08.083.

[26] S.Y. Lee, A. Hille, C. Frias, B. Kater, B. Bonitzki, S. Wolfl, H. Scheffler, A. Prokop, R. Gust, [NiII(3-OMe-salophene)]: A Potent Agent with Antitumor Activity, J. Med. Chem. 53 (2010) 6064–6070, https://doi.org/10.1021/jm100459k.

[27] I. Giannicchi, R. Brissos, D. Ramos, J. Lapuente, J.C. Lima, A.D. Cort, L. Rodriguez, Substituent effects on the biological properties of Zn-Salophen complexes, Inorg.Chem. 52 (2013) 9245–9253, https://doi.org/10.1021/ic4004356.

[28] L. Lecarme, E. Prado, A.D. Rache, M.L.N. Travers, R. Bonnet, A. Heyden, D. Van, F. Thomas, Interaction of Polycationic Ni(II)-Salophen Complexes with G-

Quadruplex DNA, Inorg. Chem. 53 (2014) 12519–12531, https://doi.org/10.1021/ic502063r.
[29] V.G. Sankareswari, D. Vinod, A. Mahalakshmi, M. Alamelu, G. Kumaresan, R. Ramaraj, S. Rajagopal, Interaction of oxovanadium(IV)–salphen complexes with bovine serum albumin and their cytotoxicity against cancer, Dalton Trans. 43 (2014) 3260–3272, https://doi.org/10.1039/c3dt52505h.
[30] K. Sakthikumar, R.V. Solomon, J.D. Raja, Spectro-electrochemical assessments of DNA/BSA interactions, cytotoxicity, radical scavenging and pharmacological implications of biosensitive and biologically active morpholine-based metal(ii) complexes: a combined experimental and computational investigation, RSC Adv. 9 (2019) 14220–14241, https://doi.org/10.1039/c8ra09218d.
[31] A. Mathavan, A. Ramdass, S. Rajagopal, A spectroscopy approach for the study of the interaction of Oxovanadium(IV)-Salen complexes with proteins, J. Fluoresc. 25 (2015) 1141–1149, https://doi.org/10.1007/s10895-015-1604-3.
[32] G. Balakrishnan, T. Rajendran, K.S. Murugan, M. Ganesan, V.K. Sivasubramanian, S. Rajagopal, Synthesis, photophysics and the binding studies of rhenium(I) diimine surfactant complexes with serum albumins: a spectroscopic and docking study approach, J. Luminesc. 205 (2019) 51–60, https://doi.org/10.1016/j.jlumin.2018.08.078.
[33] J. Liu, Y. He, D. Liu, Y. He, Z. Tang, H. Lou, Y. Huo, X. Cao, Characterizing the binding interaction of astilbin with bovine serum albumin: a spectroscopic study in combination with molecular docking technology, RSC Adv. 8 (2018) 7280–7286, https://doi.org/10.1039/c7ra13272g.
[34] G. Ayyannan, M. Mohanraj, G. Raja, N. Bhuvanesh, R. Nandhakumar, C. Jayabalakrishnan, Design, synthesis, structure and biological evaluation of new palladium(II) hydrazone complexes, Inorg. Chim. Acta 453 (2016) 562–573, https://doi.org/10.1016/j.ica.2016.09.025.
[35] (a) J. Devi, M. Yadav, D. Kumar, L.S. Naik, D.K. Jindal, Some divalent metal(II) complexes of salicylaldehyde-derived Schiff bases: synthesis, spectroscopic characterization, antimicrobial and in vitro anticancer studies, Appl. Organomet. Chem. 32 (2018) 4693–4715, https://doi.org/10.1002/aoc.4693;
(b) S. Dey, K. Pal, K. Jana, C. Sinha, Effect of -OMe substituent on Salicylaldehyde Schiff Base to influence the Zn_{2+} sensitivity and the Cancer cell line imaging, Chemistry Select 4 (2019) 7932–7935, https://doi.org/10.1002/slct.201901584;
(c) H. Yan, K. Zhong, Y. Lu, New Schiff base chromophores composed of salicylaldehyde and naphthalimide derivatives for ion sensor applications, Anal. Methods 11 (2019) 3597–3607, https://doi.org/10.1039/c9ay01035a.
[36] T.M. Fasina, O. Ogundele, F.N. Ejiah, C.U. Dueke-Eze, Biological activity of copper(II), cobalt(II) and nickel (II) complexes of schiff base derived from O-Phenylenediamine and 5-bromosalicylaldehyde, Int. J. Biol. Chem. 6 (2012) 24–30, https://doi.org/10.3923/ijbc.2012.24.30.
[37] Y. Shao, Z. Gan, E. Epifanovsky, A.T.B. Gilbert, M. Wormit, J. Kussmann, X. Feng, Advances in molecular quantum chemistry contained in the Q-Chem 4 program package, Mol. Phys. 113 (2014) 184–215, https://doi.org/10.1080/00268976.2014.952696.
[38] K. Hui, J.D. Chai, SCAN-based hybrid and double-hybrid density functionals from models without fitted parameters, J. Chem. Phys. 144 (2016) 044114–044122, https://doi.org/10.1063/1.4940734.
[39] M. Modrzejewski, G. Chalasinski, M.M. Szczesniak, Assessment of newest meta-GGA hybrids for late transition metal reactivity: fractional charge and fractional spin perspective, J. Phys. Chem. C 123 (2019) 8047–8056, https://doi.org/10.1021/acs.jpcc.8b07394.
[40] B.P. Pritchard, D. Altarawy, B. Didier, T.D. Gibson, T.L. Windus, A New basis set exchange: an open, up-to-date resource for the molecular sciences community, J. Chem. Inf. Model. 59 (2019) 4814–4820, https://doi.org/10.1021/acs.jcim.9b00725.
[41] O. Trott, A.J. Olson, Software news and update AutoDock Vina: improving the speed and accuracy of docking with a New scoring function, efficient optimization and multithreading, J. Comput. Chem. 31 (2010) 455–461, https://doi.org/10.1002/jcc.21334.
[42] A. Bujacz, Structures of bovine, equine and leporine serum albumin, Acta Crystallogr. D Biol. Crystallogr. 68 (2012) 1278–1289, https://doi.org/10.1107/s0907444912027047.
[43] F. Denizot, R. Lang, Rapid colorimetric assay for cell growth and survival modifications to the tetrazolium dye procedure giving improved sensitivity and reliability, J. Immunol. Methods 89 (1986) 271–277, https://doi.org/10.1016/0022-1759(86)90368-6.
[44] M. Mohammadikish, Green synthesis of nanorod Ni(salen) coordination complexes using a simple hydrothermal method, Cryst. Eng. Comm. 16 (2014) 8020–8026, https://doi.org/10.1039/c4ce01009d.
[45] A. Akbari, Z. Alinia, Comparative Analysis of the Ni (II) Complex of the N, N′ -Bis-(4-Hydroxysalicylidene)-1, 2-Diaminoethane: Combined Experimental and Theoretical Study(DFT/PW91), Comput. Res. 1 (2013) 19–26, https://doi.org/10.13189/cr.2013.010201.
[46] B.B. Mahapatra, R.R. Mishra, A.K. Sarangi, Synthesis, characterisation, XRD, molecular modelling and potential antibacterial studies of co(II), Ni(II), cu(II), Zn(II), cd (II) and hg(II) complexes with bidentate azodye ligand, J. Sau. Chem. Soc. 20 (2016) 635–643, https://doi.org/10.1016/j.jscs.2013.07.002.
[47] X. Liang, J. Jiang, X. Xue, L. Huang, X. Ding, D. Nong, H. Chen, Lixia Pan, Z. Ma, Synthesis, characterization, photoluminescence, anti-tumor activity, DFT calculations and molecular docking with proteins of zinc(II) halogen substituted terpyridine compounds, Dalton Trans. 48 (2019) 10488–10504, https://doi.org/10.1039/c8dt04924f.
[48] M.N. Arshad, A.M. Al-Dies, A.M. Asiri, M. Khalid, A.S. Birinji, K.A. Al-Amry, A.A.C. Braga, Synthesis, crystal structures, spectroscopic and nonlinear optical properties of chalcone derivatives: A combined experimental and theoretical study, J. Mol. Struct. 1141 (2017) 142–156, https://doi.org/10.1016/j.molstruc2017.03.090.
[49] M.N. Tahir, M. Khalid, A. Islam, S.M. Ali Mashhadi, A.A.C. Braga, Facile synthesis, single crystal analysis and computational studies of sulfanilamide derivatives, J. Mol. Struct. 1127 (2016) 766–776, https://doi.org/10.1016/j.molstruc.2016.08.032.
[50] R. Parthasarathi, V. Subramanian, D.R. Roy, P.K. Chattaraj, Electrophilicity index as a possible descriptor of biological activity, Bioorg. Med. Chem. 12 (2004) 5533–5543, https://doi.org/10.1016/j.bmc.2004.08.013.
[51] E. Atrian-Blasco, S. Gascon, M.J. Rodriguez-Yoldi, M. Laguna, E. Cerrada, Novel gold (I) Thiolate derivatives synergistic with 5-fluorouracil as potential selective anticancer agents in Colon Cancer, Inorg. Chem. 56 (2017) 8562–8579, https://doi.org/10.1021/acs.inorgchem.7b01370.
[52] D.B. Wetlaufer, Ultraviolet spectra o f proteins and amino acids, Adv. Protein Chem. 17 (1963) 303–390, https://doi.org/10.1016/S0065-3233(08)60056-X.
[53] H.A. Benesi, J.H. Hildebrand, A spectrophotometric investigation of the interaction of iodine with aromatic hydrocarbons, J. Am. Chem. Soc. 71 (1949) 2703–2707, https://doi.org/10.1021/ja01176a030.
[54] H. Yu, W. Zhang, Q.Yu, F-P. Huang, H-D. Bian, H. Liang, Ni(II) complexes with Schiff Base ligands: preparation, Characterization, DNA/Protein Interaction and Cytotoxicity Studies, Molecules 22 (2017) 1772–1793. doi:https://doi.org/10.3390/molecules22101772.
[55] a M.M.V. Ramana, R. Betkar, A. Nimkar, P. Ranade, B. Mundhe, S. Pardeshi, Synthesis of a novel 4H-pyran analog as minor groove binder to DNA using ethidium bromide as fluorescence probe, Spectrochim. Acta A 152 (2016) 165–171, https://doi.org/10.1016/j.saa.2015.07.037;
(b) J. Bhuvaneswari, P.M. Mareeswaran, S. Shanmuga sundaram, S. Rajagopal, Protein binding studies of luminescent rhenium(I) diimine complexes, Inorg. Chim. Acta 375 (2011) 205–212, https://doi.org/10.1016/j.ica.2011.05.009.
[56] M. Mallappa, B.G. Gowda, J.I. Gowda, R. Rengaswamy, Spectroscopic, voltammetry and molecular docking study of binding interaction of antipsychotic drug with bovine serum albumin, J. Electrochem. Sci. Eng. 6 (2016) 155–164, https://doi.org/10.5599/jese.205.
[57] F. Jalali, P.S. Dorraji, Electrochemical and spectroscopic studies of the interaction between the neuroleptic drug, gabapentin and DNA, J. Pharma. Biomed. Anal. 70 (2012) 598–601https://doi.org/10.1016/j.jpba.2012.06.005.
[58] J. Yu, Y. Zhou, I. Tanaka, M. Yao, Roll: a new algorithm for the detection of protein pockets and cavities with a rolling probe sphere, Bioinformatics 26 (2010) 46–52, https://doi.org/10.1093/bioinformatics/btp599.
[59] M. Sankarganesh, J. Dhaveethu Raja, N. Revathi, R.V. Solomon, R. Senthil Kumar, Gold(III) complex from pyrimidine and morpholine analogue Schiff base ligand: synthesis, characterization, DFT, TDDFT, catalytic, anticancer, molecular modeling with DNA and BSA and DNA binding studies, J. Mol. Liq. 294 (2019)https://doi.org/10.1016/j.molliq.2019.111655 111655–11166.